JOURNAL OF THERMOPHYSICS AND HEAT TRANSFER
Vol. 10, No. 1, January–March 1996

Terrestrial Solar-Pumped Iodine Gas Laser with Minimum Threshold Concentration Requirements

C. K. Terry,* J. E. Peterson,† and D. Y. Goswami‡
University of Florida, Gainesville, Florida 32611

A t-C_4F_9I iodine gas laser pumped by concentrated uv terrestrial solar radiation was designed and built. The laser consists of an optical resonator cavity, a blowdown lasant gas flow system, and a parabolic trough reflector. The optical resonator design was based on a mathematical model that used iodine gas kinetic rate equations to predict threshold pumping power, available pumping power, and laser output power for various dimensions. An optimum design for this demonstration project was selected to minimize lasing threshold solar concentration to 40 suns, and retain a 15-min run time with our limited lasant supply. Output power was not optimized, and is predicted to be low (20 mW). An estimate of local spectral uv terrestrial irradiation was developed from band and total irradiation measurements. It was used to estimate solar concentration required to initiate lasing and laser output power. The laser, gas flow system, and parabolic trough collector were built and evaluated. Irradiation at the parabolic trough's focus (where the laser tube was placed) was measured for directional and total irradiation. These measurements showed an average solar concentration of 15–20 suns below threshold. The study establishes the feasibility of terrestrial solar-pumped iodine lasers with low threshold, and simple, stable, and controllable lasant flow systems.

Nomenclature

A_c = aperture of primary solar collector, m^2
A_i = irradiated laser tube surface area, πDL_m, m^2
A_{34} = Einstein A coefficient of the 3–4 hyperfine level transition, s^{-1}
c = speed of light, m/s
D = laser tube diameter, m
h = Planck's constant, J s/photon
I = atomic iodine
I^* = excited atomic iodine
L_m = irradiated length of laser tube, m
P_a = available pump power, Eq. (1), W
P_{out} = output power, Eq. (7), W
P_{th} = threshold pump power, Eq. (4), W
p = pressure, Pa or torr
R = radical molecule associated with the atomic iodine
R_1, R_2 = reflectivity of 100% and output coupled mirrors
SC = solar concentration, suns
T = temperature, K
T_i = transmissivity of lasant medium and Brewster windows
W = width of parabolic trough, m
W_p = pumping probability, Eq. (2)
γ = total decay rate of upper level atom, s^{-1}
$\Delta\nu_d$ = Doppler linewidth of the 3–4 transition, s^{-1}
η_p = quantum yield
ι = ambient solar spectral irradiation, W/m^2 nm
λ = wavelength, m
λ_p = pumping wavelength, m
ν_e = midband emission frequency, s^{-1}
σ_a = lasant spectral absorption cross section, Eq. (8), cm^2
σ_e = lasant spectral emission cross section, cm^2
[ ] = molecular density, mol/m^3
$\forall$ = volume of laser irradiated, $\pi D^2 L_m/4$, m^3

Presented as Paper 94-4025 at the AIAA 29th Intersociety Energy Conversion Engineering Conference, Monterey, CA, Aug. 7–12, 1994; received March 10, 1995; revision received July 14, 1995; accepted for publication July 17, 1995.

*Research Assistant, Solar Energy and Energy Conversion Laboratory, Department of Mechanical Engineering.
†Assistant Professor, Solar Energy and Energy Conversion Laboratory, Department of Mechanical Engineering.
‡Professor and Director, Solar Energy and Energy Conversion Laboratory, Department of Mechanical Engineering.

Introduction

THE present work addresses the design of a small power solar-pumped iodine gas laser. The work is built on a foundation of work by NASA for space-based solar laser pumping. While solar-pumped solid-state lasers, principally Nd:YAG crystals, have been studied by other groups, we believe our work to be the first addressing a terrestrial solar-pumped gas laser. The solid-state lasers have a better overlap of the absorption cross section with spectral terrestrial insolation, and therefore, have higher potential efficiencies than the iodine gas studied in our work. This lower efficiency of iodine gas has distracted others from studying iodine gas as a potential lasant medium. However, using efficiency alone as the criterion to evaluate lasants has the implicit assumption that the collection of more solar irradiation will cost proportionately more, just as in the case of fossil fuels. In reality, the solar irradiation is free, and the true expense involved is in the construction of a suitable solar reflection system to direct the concentrated solar energy to the lasant medium. Iodine gas pumps at low thresholds: well under 100 suns, a value easily obtainable even by troughs originally intended for heating water. On the other hand, the high efficiency solid-state lasers require extremely specialized optical grade equipment, and 84,000 suns to pump. The difficulty of generating such high concentrations offsets the apparent advantage of efficiency of the solid-state lasers. Other advantages of the iodine gas laser as compared to solid-state solar-pumped lasers are that it is easily cooled (by simply flowing the gas through the laser tube during operation) and is inexpensive to upgrade to high power (the gas will expand to fill any size oscillation cavity).

Impact of this project will be seen in several areas of interest, particularly in the development of alternative energy sources for terrestrial and extraterrestrial use. Iodine lasers have many potential applications in the areas of manufacturing and materials processing. For example, iodine gas lases in the infrared (IR) at 1315 nm, a wavelength that couples well with the surface of most metals. It is thus suitable for surface hardening and modification of metals, for welding, drilling, and for cutting. Other manufacturing applications could include cutting of ceramics, micromachining, and laser deposition of nonmetallic coatings on metal surfaces. The iodine lasing wavelength is good for use in fiber optic delivery systems (it typically exhibits better transmission than the YAG or He-Ne laser), and for monitoring of atmospheric pollutants (as it is optically safer than the YAG laser). One of the newer applications that has been suggested is solar hazardous waste detoxification.

The scope of this project covered the design and development of a demonstration laser using the limited amount of iodine gas available, and with a minimum threshold requirement. Anticipated output power was thus a secondary consideration and is predicted to be low for this system. However, our system scaling and optimization studies show potential continuous wave power of up to 90 W using commercially available solar reflectors.[1]

The development of solar-pumped lasers began in the early 1960s, not long after the invention of the laser itself.[2] Solid-state lasers, pumped by concentrated terrestrial sunlight, have been built by various researchers.[2-9] Solid crystals pumped include Nd:YAG, Nd:Cr:GSGG, and Er, Tm, Ho:YAG. The solid-state lasant crystals are attractive lasant media as they have a good overlap of their absorption cross section with the terrestrial solar spectrum. However, they also have many drawbacks. Growing laser-quality crystals of usable size is difficult. Since output power is directly proportional to the amount of lasant material, solid-state laser power is ultimately limited by maximum crystal size. The waste heat created by the concentrated solar irradiation causes thermal lensing within the laser crystal, which can distort the beam output. The most significant problem, however, is the formation of thermal gradients within the crystal that lead to fracture. Cooling the lasant crystal to 77 K (using liquid nitrogen) alleviates this problem (YAG crystal thermal conductivity significantly increases at low temperature, Benmair et al.[7]), but does not completely solve it. In addition to cooling the YAG crystal to 77 K, Benmair et al. were forced to physically block the solar irradiation 80% of the time, operating in a quasicontinuous mode. These cooling requirements significantly reduce the overall laser efficiency and must be considered when comparing various lasant media. End pumping configurations have even more significant cooling problems, as extremely high concentrations of solar radiation are required to pump the entire length of the crystal.[9]

A gas lasant is advantageous for solar pumping because it does not have a fixed structure, is less affected by heat buildup, and can be continuously cycled through the pumped zone to prevent heat buildup. Iodine gas lasant absorbs solar irradiation only at wavelengths in its pumping region, so that the only thermal energy generated is from losses during the lasant reaction. As this gas lasant has a low threshold pumping power requirement, the problems with heat buildup are significantly reduced. Many iodine lasants have a spectral absorption cross section that overlaps with the extraterrestrial solar spectrum and have been successfully pumped on Earth by a solar simulator with an AM0 spectral distribution of irradiation.[10-16] The only iodine gas lasant suitable for terrestrial pumping though is t-C_4F_9I, as the absorption cross section is red-shifted relative to other iodine lasants, resulting in an overlap with terrestrial insolation. The absorption cross section and estimates of AM1 spectral irradiation distributions are seen in Fig. 1.

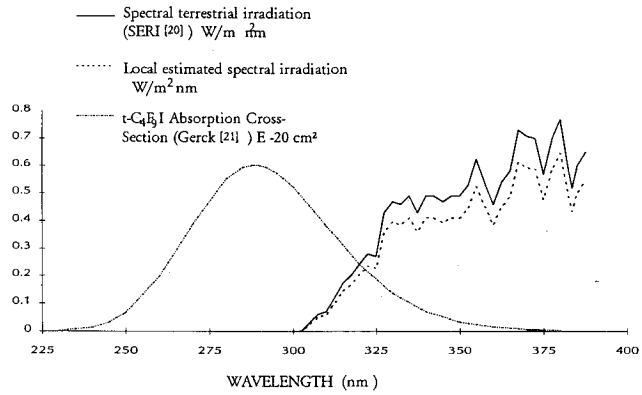

Fig. 1 Lasant absorption cross section and spectral irradiation.

A solar-pumped laser using an iodine lasant was examined theoretically and experimentally at NASA-Langley (Hwang and Tabibi[13]). The system utilized an Argon solar simulator (AM0 spectral distribution), which pumped a flowing iodine gas lasant over a 20 cm length. The optical resonator cavity was 1.8 m long and the gas was driven by a simple blowdown system. A series of tests was conducted using a variety of lasants, flow velocities, operating pressures, and output couplings. In conjunction with these tests, a simplified mathematical model of iodine gas kinetic rate equations was developed for use in scaling and predicting the performance, and is used in our next analysis.

System Mathematical Modeling

In the present work, the rate equation model of Hwang and Tabibi[13] was used to predict the output power of a t-C_4F_9I iodine gas laser pumped by concentrated terrestrial solar radiation. Hwang and Tabibi used n-C_3F_7I as the lasant gas and predicted power output as a function of physical parameters such as operating pressure, output coupling, and available pumping power. The model was modified by replacing the solar simulator spectral irradiation profile with our data estimating local uv terrestrial irradiation and by using the material properties of t-C_4F_9I instead of n-C_3F_7I.

The available pumping power P_a is the irradiation absorbed by the lasant in the pumping band and is calculated as

$$P_a/\forall = W_p(hc/\lambda_p)[RI] \tag{1}$$

where W_p is the potential for lasant molecule's excitation by an irradiating photon. Pumping probability is calculated by integrating across the spectrum

$$W_p = \frac{1}{[RI]}\frac{A_t}{\forall} \times \int_0^\infty \eta_p(\lambda)[SC\ i(\lambda)]\left(\frac{\lambda}{hc}\right)\{1 - \exp[-\sigma_a(\lambda)[RI]D]\}\,d\lambda \tag{2}$$

The quantum yield η_p, a measure of how well excited atoms are utilized in the laser transition, is approximately 1.0.[17] Estimates of our local spectral irradiation $\iota(\lambda)$ are discussed later. Equation (1) was rewritten for design purposes as

$$\frac{P_a}{\forall} = \pi D L_m \int_0^\infty \eta_p[SC\ i(\lambda)]\{1 - \exp[-\sigma_a(\lambda)[RI]D]\}\,d\lambda \tag{3}$$

This equation shows that available pumping power can be optimized by variation of laser tube diameter and lasant density.

To determine the solar concentration required to initiate lasing, the threshold pumping power was calculated as[18]

$$\frac{P_{th}}{\forall} = \left\{\frac{-2[\not{\eta} T_i + (\not{\eta} R_1 + \not{\eta} R_2)]}{\eta_p}\right\}\left(\frac{hc}{\lambda_p}\right)\left(\frac{\gamma}{2L_m\sigma_e}\right) \quad (4)$$

Advantages of t-C_4F_9I include a relatively low decay rate (γ = 7.69 Hz) and high quantum yield (η_p = 1.0).[19] Lasant medium and Brewster window transmissivity were estimated at 0.98. The stimulated emission cross section σ_e is calculated as

$$\sigma_e = (\tfrac{7}{12})(A_{34}/4x^2)\{(\lambda^2/\Delta\omega_d) + K(p - 20)[14 \times 10^7]\} \quad (5)$$

where A_{34} was estimated as 5.1 s^{-1}, and the Doppler broadened linewidth as 250 MHz. The final term of Eq. (5) accounts for pressure broadening effects. The pressure broadening constant is not well determined for t-C_4F_9I, but was roughly approximated at $K = 0$ when $p < 20$ torr, and $K = 1.0$ when $p > 20$ torr.[13]

Finally, laser output power is predicted as

$$\frac{P_{out}}{\forall} = [h\nu_e][\gamma]\left[\frac{-\not{\eta} R_2}{-2\not{\eta} T_i - \not{\eta} R_1 - \not{\eta} R_2}\right]([I^*] - [I^*]_{ent}) \quad (6)$$

where $[I^*] = W_p[RI]/\gamma$. $[I^*]_{ent}$ accounts for nonusable entry length effects, and for pumping well above threshold, is approximately equal to the threshold excitation level.

The effects of oscillation cavity dimensions and gas operating conditions on P_a, P_{th}, and P_{out}, were predicted using Eqs. (3), (4), and (6). The goal of this project was to develop a demonstration system using a simple concentrator and limited lasant supply. Emphasis was placed on designing an oscillation cavity to 1) minimize the threshold pumping power and 2) retain run times long enough for optical cavity alignment. The laser tube length and diameter, operating pressure, and output coupling (reflectivity) were varied to find an optimum value with respect to these two criteria. For this demonstration system, output power was not an optimization criterion.

Estimates of Local Spectral Irradiation in the uv Band

The tracking pyronometer at the University of Florida Solar Energy and Energy Conversion Laboratory measures direct total insolation. Because the iodine gas pumps in the uv (midband terrestrial pumping wavelength is approximately 325 nm), accurate prediction of irradiation in the uv band was essential to prediction of threshold solar concentrations by Eqs. (1) and (2). A database of direct total and of direct uv (300–380-nm) measurements was built and used to predict the uv spectral irradiation as a function of total insolation measured by the pyronometer. Measurements were taken during various weather conditions at times within 2 h of solar noon. As can be seen in Table 1, the ratio of uv band average to total found locally (3.3%) compares favorably with the SERI[20] ratio (3.2%), but the local total and uv averages are lower. The local estimated spectral irradiation shown in Fig. 1 was constructed by scaling the SERI spectral profile with a linear correction factor until the power flux in the band from 300 to 380 nm matched the local average flux indicated in Table 1. The plot shown was used to estimate the spectral irradiation $\iota(\lambda)$, in estimates of available pumping power [Eq. (3)].

System Descriptions: Design, Assembly, and Operation

The laser system can be divided into three components: 1) the optical resonator, 2) the gas flow system, and 3) the solar reflector. Figure 2 is a schematic of the optical resonator (consisting of the laser tube, Brewster windows, and two mirrors), and the lasant flow system (supply and retrieval flasks, flow meter, pressure and temperature sensors, valves, and vacuum pump).

Table 1 Local total and uv direct irradiation

Date and time	Local direct total irradiation, W/m²	Local direct uv band irradiation, 300–380 nm, W/m²	Ratio of uv band to total irradiation, %
8-5-93, 10:30	465	16.7	3.6
8-5-93, 12:55	534	19.8	3.7
8-6-93, 11:30	586	20.6	3.5
8-6-93, 1:00	648	21.1	3.3
8-12-93, 1:25	800	28.5	3.6
8-24-93, 1:00	750	23.5	3.1
10-1-93, 12:00	870	23.5	2.7
10-22-93, 11:30	930	24.2	2.6
Local average	660	21.7	3.3
SERI[20]	879	27.5	3.2

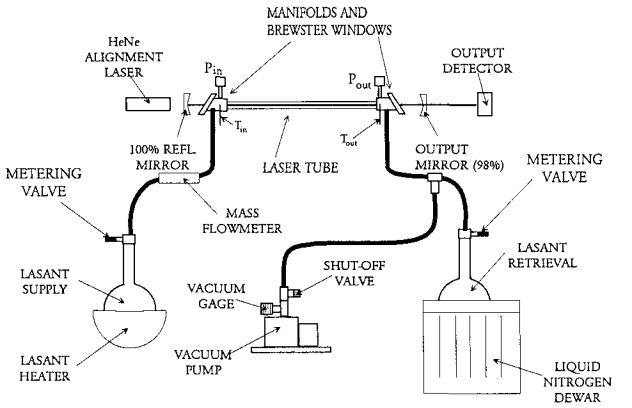

Fig. 2 Optical resonator cavity and gas delivery system.

Optical Resonator Cavity

The lasant flow velocity was considered first in the optical resonator design since this factor, along with the laser tube diameter, fixed the laser's maximum operating time. The minimum time needed for optical alignment and system stabilization was estimated at 15 min. With 200 g of lasant available, a 6 m/s minimum lasant flow velocity,[13] and operating pressure of 20 torr, the largest allowable laser tube diameter was 1.0 cm. This largest tube diameter was chosen to maximize the cross-sectional target area and reduce optical alignment problems. The tube wall was chosen at 1 mm to minimize transmissivity losses.

Figure 3 shows required solar concentration to initiate lasing as a function of tube length for a 1-cm-diam tube operating at 20 torr. This threshold concentration requirement is determined by finding the solar concentration (SC) necessary for the available pumping power [Eq. (1)] to reach the threshold power level predicted by Eq. (4). For a 1-cm-diam tube, 1.7-m-long tube is predicted to require 50 suns to initiate lasing. A 2-m length was chosen, with a threshold solar concentration predicted below 40 suns. As seen in Fig. 3, longer tube lengths had only a small affect on required concentration, but would significantly increase difficulties in aligning the optical resonator cavity. Figure 4 shows threshold solar concentration and output power (for 1-cm-diam, 2-m length tube with output coupled mirror of 98% reflectivity) as a function of operating pressure. The optimum operating pressure is shown to be 20 torr. From pressures of 5–20 torr, it is seen that the threshold concentration remains approximately constant, while output power increases due to the availability of

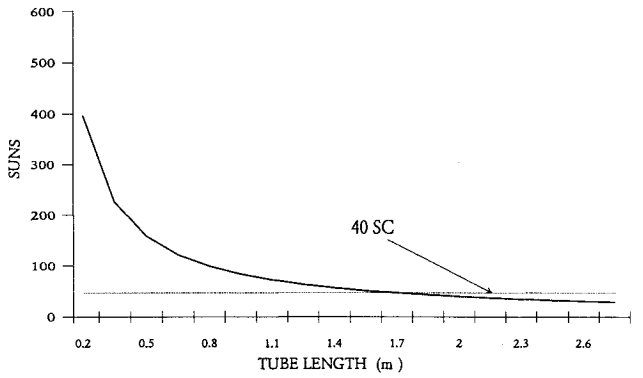

Fig. 3 Threshold solar concentration as a function of 10-mm-diam tube length operating at 20 torr.

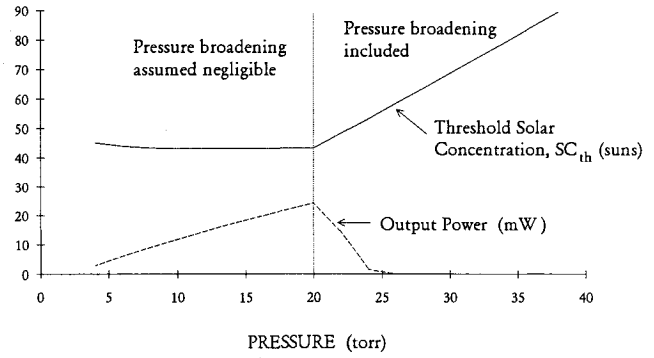

Fig. 4 Threshold concentration and output power as a function of pressure for a laser tube of i.d. 1 cm, length 2 m, and 98% output coupling.

more molecules to be pumped. At pressures above 20 torr, the effects of pressure broadening are included in Eqs. (4) and (5) ($K = 1$), causing an abrupt increase in threshold concentration, and decrease in output power.

The optical resonator consists of the laser tube, two mirrors, and two optical grade quartz Brewster windows contained in manifolds at each end of the laser tube. The parabolic reflector, laser tube, and manifold are seen in Fig. 5, and a detail of a manifold, Brewster window, and laser mirror is seen in Fig. 6. The manifolds were designed to allow the iodine gas to enter from below and pass into the laser tube without interfering with the laser optical path. Two optical-grade mirrors (100% reflective and <100% reflective) were used, and a 4-mW HeNe laser was used for mirror and optical cavity alignment. All optical components were mounted to a precision optical rail that ran beneath the parabolic trough and parallel to its focal axis. The optical cavity and mirror alignment was most easily performed at dusk when the HeNe laser was easily visible, as well as its reflections off the mirror surfaces (the mirrors were of low reflectivity at 633 nm, the HeNe laser wavelength). The reflections from the mirrors were used to autocollimate these reflectors and the laser tube.

Gas Delivery System

The lasant flow system was designed to allow for an adjustable, monitored flow that could be safely contained and manipulated. The flow system had to maintain a high vacuum (<0.001 torr) and be assembled of components that are easily connected and disconnected. Additionally, all components had to be able to survive high heat and humidity or be easily detachable for storage elsewhere. The components on the supply side were the supply flask that contained the lasant, a metering valve used for flow control, a flask heater for increasing lasant temperature, and a low-pressure-drop (<1 torr) mass flow meter (Hastings U-5KM) used for lasant mass flow rate and velocity. On the opposite end the lasant was collected in a flask immersed in liquid nitrogen that was used to reduce the lasant partial pressure to near zero. The solidifying lasant created a pressure drop across the system that drove the lasant flow. Also connected to this retrieval line was the high-vacuum pump used to establish the initial vacuum of 10^{-6} torr (vacuum measured by Edwards AIM-S-NW25 active inverted magnetron gauge; 10^{-2}–10^{-8} torr). Once the vacuum was established, the pump was isolated from the flow by a shutoff valve. Inlet and outlet pressures and temperatures were monitored at the appropriate manifolds by high-vacuum manometers (Edwards model 622A barocel absolute pressure transducer; 100-torr full scale and model 1570 pressure monitor) and type K thermocouple probes.

The first step in establishing lasant flow was to evacuate the flow system to eliminate quenching agents, primarily N_2 and O_2. Once the vacuum (<1 mtorr) had been established, the retrieval flask was chilled by submerging it in liquid nitrogen. The valve to the lasant container was opened and lasant introduced into the system at the supply side. Mass flow rate and pressure data were collected continuously during operation, to calibrate the mass flow meter and to determine the gas flow stability and controllability. For these tests, the lasant did not require heating since the lasant velocity was high enough to prevent significant iodine buildup. Data monitored in real time included inlet and outlet pressures and

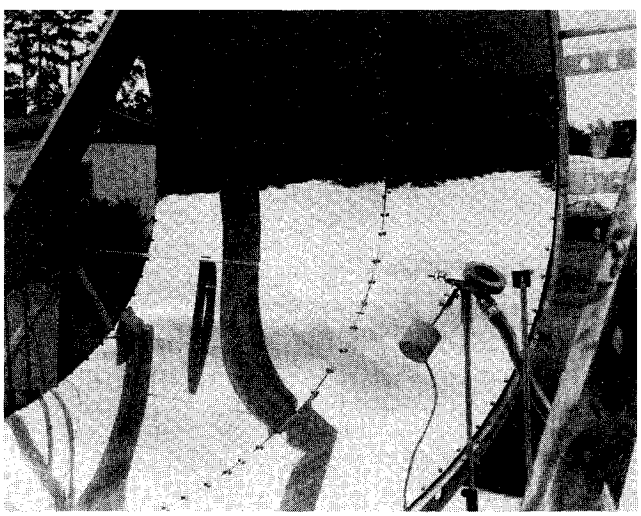

Fig. 5 Parabolic solar reflector, laser tube, and manifold.

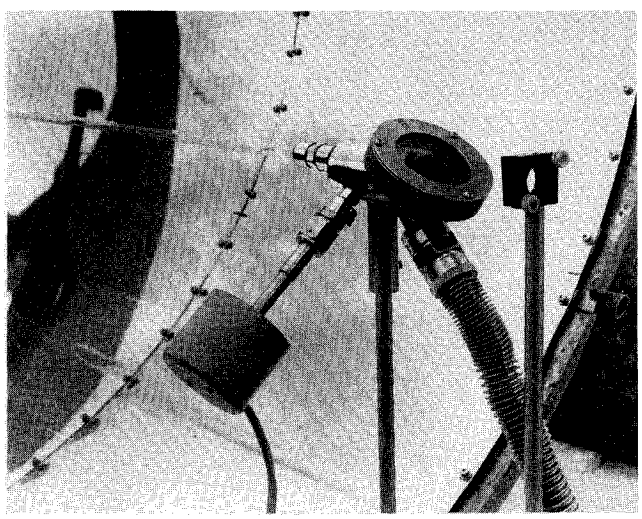

Fig. 6 Detail of manifold, pressure transducer, Brewster window, and laser mirror.

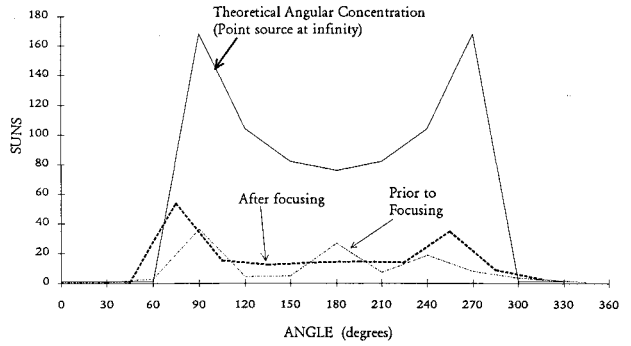

Fig. 7 Solar concentration as a function of angle at a 5-mm radius about the parabolic reflector axis.

temperatures, mass flow rate, total insolation, and output power. Data readings were linked to a computer in order to record and process test data.

Solar Reflector, and Estimates of uv Irradiation

A parabolic concentrator trough (dimensions length = 2 m; width = 2 m) was the primary reflector. It was placed in an east–west alignment to eliminate tracking requirements once the daily declination angle had been set. The trough surface was covered with 3M Alumilux SA-85, a specularly reflecting aluminum film with good reflectivity in the uv portion of the spectrum (78%). A wooden parabolic template was cut to the ideal cross-sectional parabolic profile ($y = 0.0169x^2$) and indicated adjustments made to the reflector surface. Once this focusing was completed, a series of measurements was taken to find spectral irradiation in the pumping band incident at the laser tube.

A low level power meter (coherent 210 thermal disk sensor) was used to measure total intensity of irradiation at the concentrator axis at the radius of the laser tube. The power meter's sensor head was encased in the Alumilux reflective film, and a small aperture (2 by 3 mm) of the sensor surface exposed. The sensor head aperture was rotated about the trough axis at known radius to measure solar irradiation as a function of angle. Solar concentration as a function of angle at a 5-mm radius is seen in Fig. 7. Total solar irradiation incident at the tube surface was found by integration of these angular measurements over 360 deg. Irradiation estimates were independently verified by use of a bulk energy balance. A 10-mm-diam copper tube was mounted at the trough focal axis. The tube surface was coated with high absorptivity 3M Nextel black velvet coating. Using known spectral properties of all surfaces and the ambient total insolation, an energy balance predicted the solar concentration level required to produce the measured temperature of the copper rod. Irradiation estimates from the two methods differed by a maximum of 20%.

While the laser was predicted to reach threshold at approximately 40 suns, because of large surface errors of the reflector, the trough average concentration was only 20 suns (Fig. 7). Therefore, lasing could not be achieved with the present setup.

Conclusions and Recommendations

This study has established a number of facts about the possibilities for terrestrial solar-pumped iodine lasers. The most significant fact is that modeling results confirm the feasibility of a working laser that has reasonably low (40 suns) threshold flux requirements. Additionally, a simple, stable, controllable flow system with basic instrumentation can be easily assembled. Also, it was proven that an acceptably accurate uv insolation profile could be approximated using a combination of established spectral data and local broadband data. Finally, it was possible to use the computational model and insolation data to predict laser performance and optimize the laser's design.

To produce a working laser, the remaining task is to incorporate the use of a sufficient solar concentration system. One alternative would be to use a concentrator built specifically for these purposes and constructed in such a way as to eliminate focusing problems caused by surface slope errors and other deviations. Another alternative is to add a larger primary concentrator that would collect and redirect enough solar power to produce fluxes well in excess of threshold requirements.

In summary, with its low threshold requirements and operational simplicity, the terrestrial solar-pumped iodine gas laser shows high potential for becoming operational. Compared to other systems under development, it is a viable alternative that possesses a number of significant advantages. With the aid of a concentration system capable of producing higher power fluxes, the laser should prove to be an effective research tool.

Acknowledgments

The concentrator's reflective film was donated by the 3M Corporation. The work was funded in part by Engineering Division/ASME Division Research Initiation Award RI-A-93-05 and General Electric Young Faculty Grant 90072001. Invaluable information and advice were also supplied by J. H. Lee, B. M. Tabibi, and other members of the NASA-Langley solar laser research staff. This support is greatly appreciated.

References

[1]Terry, C. K., Peterson, J. E., and Goswami, D. Y., "Feasibility of an Iodine Gas Laser Pumped by Concentrated Terrestrial Solar Radiation," *Solar Engineering*, 1995, pp. 671–678.

[2]Young, C. G., "A Sun-Pumped CW One Watt Laser," *Applied Optics*, Vol. 5, No. 6, pp. 993–997.

[3]Arashi, H., Oka, Y., Sasahara, N., Kaimai, A., and Ishigame, M., "A Solar-Pumped CW 18W Nd:YAG Laser," *Japanese Journal of Applied Physics*, Vol. 23, No. 8, 1984, pp. 1051–1053.

[4]Arashi, H., and Kaneda, Y., "Solar-Pumped Laser and Its Second Harmonic Generation," *Solar Energy*, Vol. 50, No. 5, 1993, pp. 447–451.

[5]Weksler, M., and Shwartz, J., "Solar-Pumped Solid-State Lasers," *IEEE Journal of Quantum Electronics*, Vol. 24, No. 6, 1988, pp. 1222–1228.

[6]Noter, Y., Oron, M., Shwartz, J., Weksler, M., and Yogev, A., "Solar-Pumped Nd:Cr:GSG Laser," *SPIE 6th Meeting in Israel on Optical Engineering*, Vol. 1038, 1988, pp. 512–520.

[7]Benmair, R. M. J., Kagan, J., Kalisky, Y., Noter, Y., Oron, M., Shimony, Y., and Yogev, A., "Solar-Pumped Er,Tm,Ho:YAG Laser," *Optics Letters*, Vol. 15, No. 1, 1990, pp. 36–38.

[8]Winston, R., Gleckman, P., Jenkins, D., O'Gallagher, J., and Lewandowski, A., "Ultra-High Solar Flux and Applications to Solar Pumping," *Proceedings of Solar '93, ASES Annual Conference*, 1993, pp. 225–228.

[9]Cooke, D., "Sun-Pumped Lasers: Revisiting an Old Problem with Nonimaging Optics," *Applied Optics*, Vol. 31, No. 36, 1992, pp. 7541–7546.

[10]Hwang, I. H., and Han, K. S., "A Continuously Pumped Iodine Laser Amplifier," *Optics Communications*, Vol. 84, No. 3–4, 1991, pp. 169–174.

[11]Hwang, I. H., and Lee, J. H., "Efficiency and Threshold Pump Intensity of CW Solar-Pumped Solid-State Lasers," *IEEE Journal of Quantum Electronics*, Vol. 27, No. 9, 1991, pp. 2129–2131.

[12]Hwang, I. H., Lee, J. H., and Lee, M. H., "A Long-Pulse Amplifier for Solar-Pumped Iodine Lasers," *Optics Communications*, Vol. 58, No. 1, 1986, pp. 47–52.

[13]Hwang, I. H., and Tabibi, B. M., "A Model for a Continuous Wave Iodine Laser," *Journal of Applied Physics*, Vol. 68, No. 10, 1990, pp. 4983–4989.

[14]Lee, J. H., Weaver, W. R., and Tabibi, B. M., "Perfluorobutyl Iodides as Gain Media for a Solar-Pumped Laser Amplifier," *Optics*

Communications, Vol. 67, No. 6, 1988, pp. 435–440.

[15]Tabibi, B. M., Gambo, A. M., and Venable, D. D., "Perfluoro-t-Butyl Iodide as an Alternate Laser Medium for Solar Pumping in Space," Lasers and Electro-Optics, Conf., Baltimore, MD, 1991.

[16]Tabibi, B. M., Lee, M. H., Lee, J. H., and Weaver, W. R., "Perfluorobutyl Iodides as Gain Media for a Solar-Pumped Iodine Laser Amplifier," International Conf. on Lasers, 1986.

[17]Lee, J. H., private communication, NASA Langley, Oct. 1992.

[18]Siegman, A. E., *Lasers*, Univ. Science Books, Mill Valley, CA, 1986.

[19]Brederlow, G., Fill, E., and Witte, K. J., *The High-Power Iodine Laser*, Springer–Verlag, New York, 1983.

[20]"1961–1990 Solar Radiation Data Base," SERI, TR-215-15989-12, Golden, CO, 1990.

[21]Gerck, E., Max-Planck-Institut F. Quantenoptik, MPQ Rept. 58, D-8046 Garching, 1982.